Date of publication xxxx 00, 0000, date of current version xxxx 00, 0000.

Digital Object Identifier 10.1109/ACCESS.202X.DOI

Broadband Reflectarray with High Polarization Purity for 4K and 8K UHDTV DVB-S2

DANIEL R. PRADO[1], MANUEL ARREBOLA[1], (Senior Member, IEEE,) MARCOS R. PINO[1], AND GEORGE GOUSSETIS[2], (Senior Member, IEEE)

[1]Department of Electrical Engineering, Universidad de Oviedo, Gijón, Spain (e-mail: {drprado,arrebola,mpino}@uniovi.es)
[2]Institute of Sensors, Signals and Systems, School of Engineering and Physical Sciences, Heriot-Watt University, Edinburgh, U.K. (e-mail: G.Goussetis@hw.ac.uk)

Corresponding author: Daniel R. Prado (e-mail: drprado@uniovi.es).

This work was supported in part by by the Ministerio de Ciencia, Innovación y Universidades under project TEC2017-86619-R (ARTEINE); by the Ministerio de Economía, Industria y Competitividad under project TEC2016-75103-C2-1-R (MYRADA); by the Gobierno del Principado de Asturias/FEDER under Project GRUPIN-IDI/2018/000191; by Ministerio de Educación, Cultura y Deporte / Programa de Movilidad "Salvador de Madariaga" (Ref. PRX18/00424).

ABSTRACT A broadband spaceborne reflectarray with high polarization purity is proposed for Ultra High Definition TV (UHDTV) broadcasting for direct-to-home (DTH) applications. The provided bandwidth would allow to offer DTH and other services, while the enhanced cross-polarization performance enables the improvement of a better signal-to-interference-plus-noise ratio. The broadband design procedure is based on a multi-resonant unit cell with several degrees of freedom (DoF) and an improved multi-frequency optimization algorithm. It is divided into several stages and sub-stages in order to facilitate convergence towards a broadband, contoured-beam, high-performance design, including the cross-polarization figure-of-merit in the procedure. A one-meter contoured-beam reflectarray working in a 20% frequency band with high polarization purity is presented as an example. The antenna is designed to fulfil the requirements of a European coverage for DTH UHDTV broadcasting in dual-linear polarization. The cross-polarization figure-of-merit greatly improves after the optimization procedure in the whole band, achieving values better than 37 dB in the coverage region, providing an excellent isolation between polarizations. This procedure can also be extended to other satellite applications in dual-circular polarization.

INDEX TERMS Broadband reflectarray, polarization purity, ultra high-definition TV, contoured-beam, direct broadcast satellite, crosspolar discrimination (XPD), crosspolar isolation (XPI), satellite communications

I. INTRODUCTION

One of the advantages of satellite broadcasting is the availability of a considerable amount of dedicated bandwidth with regard to terrestrial services, specially in the range of millimetre waves, which is yet to be widely exploited. Nevertheless, these extremely high frequency bands present several shortcomings, most notably attenuation due to gas absorption and atmospheric events, which still need further research [1]. Currently, TV broadcasting services are provided in the Ku-band, and may be also suitable for ultra-high definition TV (UHDTV). In fact, UHDTV with 4K and 8K resolutions has already been tested by NHK using 16- and 32-APSK in the 12 GHz band satellite channel [2]. Furthermore, the first commercial satellite to offer UHDTV is the BSAT-4a, launched in September 2017 into geostationary orbit 110° E, and being compatible with 2K, 4K and 8K resolutions. It provides the service in the frequency range 11.70 GHz–12.75 GHz [3], which corresponds to a 9% bandwidth. Terrestrial digital video broadcasting in 8K is not currently possible, although it is an ongoing research effort [4].

A key component of wireless communication systems, especially in satellite applications such as direct-to-home (DTH, see Fig. 1), is the antenna subsystem. It is often the largest device in the satellite and it converts guided waves into radiating waves in free space, and vice versa. Traditionally, parabolic reflectors and direct radiating phased arrays have been employed as spaceborne antennas [5]. Although they represent a well tested and reliable solution, they exhibit

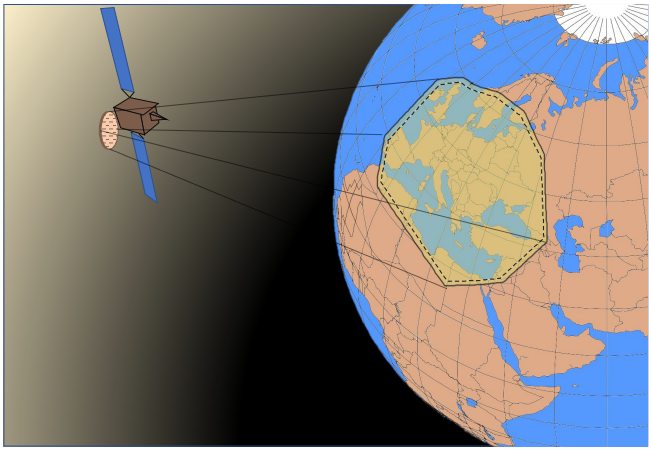

FIGURE 1. Sketch of the European coverage provided by the satellite in geostationary orbit for DTH application. The outer coverage contour takes into account typical pointing errors.

some shortcomings. Parabolic reflectors present high volume and mass, and for broadcasting applications custom moulds are manufactured for shaped reflectors. These moulds are specific for each mission and cannot be reused, considerably increasing the cost and manufacturing time. In addition, dual-gridded or Gregorian configurations are necessary to meet the cross-polarization specifications, further penalizing the volume, mass and ease of accommodation in the satellite structure. On the other hand, direct radiating phased arrays require a feeding network which may introduce high losses and complexity in the design. Reflectarray antennas [6] offer solutions to these problems. They are a class of spatially fed antennas usually comprised of a feed antenna and a flat panel comprised of a number of reflecting elements. They present low-losses and do not require complex feeding networks as phased arrays, and contoured beams can be easily generated by tuning the geometry of the elements, significantly reducing manufacturing cost and time. Furthermore, they achieve similar performances to shaped parabolic reflectors, and thanks to their flat nature, they are easily deployable, representing a cheap solution for spaceborne antennas with high performance.

There are several strategies for the design of broadband reflectarrays. One is to employ multi-resonant wideband elements, such as stacked patches [7], patches aperture-coupled to delay lines [8], or parallel dipoles [9], among others. Bandwidth may also be improved by using an artificial impedance surface in the form of sub-wavelength elements [10], although they may present some limitations when employed for very large reflectarrays for contoured-beam applications, such that they do not provide a full 360° phase-shift, which may limit the reflectarray performance. The availability of several degrees of freedom (DoF) in multi-resonant unit cells allows the optimization of the geometry at several frequencies to improve the bandwidth. Other strategies include increasing the F/D ratio, and using curved or multi-faceted reflectarrays. However, using curved or multi-faceted reflectarrays complicates the antenna structure with regard to planar reflectarrays, while increasing the F/D ratio produces a larger antenna and increases spillover for a given feed.

In addition, the cross-polarization improvement of reflectarrays requires the optimization of the whole antenna along with an accurate analysis of the unit cell. Since for high-gain applications they are typically comprised of thousands of elements, this is a very challenging task. For instance, in [11] a reflectarray was optimized in a 16% bandwidth, but only considering single circular polarization with no cross-polarization requirements. In [12] a shaped-beam reflectarray with European coverage was optimized in a 20% bandwidth, but it also works in single polarization. The same reflectarray was later optimized in [13] in dual-linear polarization with a worst minimum crosspolar discrimination (XPD_{min}) of 24.1 dB. The reflectarrays designed in [14] work in dual-linear polarization, but they were optimized only at a single frequency (monochromatic design), and thus they operate in a very narrow bandwidth. Finally, in [15] a wideband reflectarray was designed with European coverage, obtaining a crosspolar isolation better than 30 dB in a 99% of the coverage in a 9.2% bandwidth using a unit cell comprised of three layers of stacked patches. However, the design technique does not take cross-polarization requirements into account, resulting in a sub-optimal design.

In this work, we present the design of a high-performance broadband reflectarray with high polarization purity for UHDTV satellite broadcasting for DTH application. To that end, a new synthesis process is considered in this paper, that of a broadband contoured-beam reflectarray with enhanced cross-polarization performance. To achieve that goal, the stages of the dual-band design procedure developed in [16] are not suitable and they must be divided in different sub-stages. At each sub-stage, the orthogonal polarizations are optimized independently, improving convergence towards a broadband design with enhanced cross-polarization performance in the whole band. This novel methodology has been applied to the design of a dual-linear polarized reflectarray working in a 20% bandwidth in X-Ku bands in the range 10.65 GHz–13.05 GHz. The cross-polarization performance is measured by means of the figure-of-merit crosspolar discrimination (XPD) and crosspolar isolation (XPI) in the whole band. The antenna achieves a minimum copolar gain in the coverage zone of 28 dBi and a minimum XPI of at least 37 dB in a 20% bandwidth, improving the performances of other contoured-beam reflectarrays in the literature in terms of bandwidth and cross-polarization. In addition, a design precision and drift tolerance has also been carried out, showing that the optimized antenna still complies with requirements in the whole band after taking into account these phenomena. The enhanced performance allows to obtain a better signal-to-interference-plus-noise ratio, which in turn improves the spectral efficiency [17].

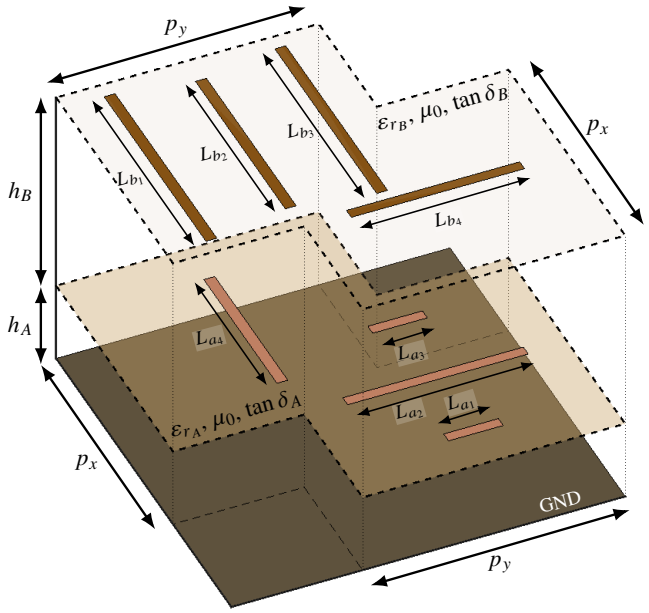

FIGURE 2. **Unit cell based on two sets of parallel dipoles in two layers of metallization employed in this work.**

II. DESIGN METHODOLOGY FOR BROADBAND PERFORMANCE

A. OVERVIEW OF THE REFLECTARRAY ANALYSIS

A complete description of the reflectarray analysis can be found in [14] and it will be briefly reviewed here. The reflectarray is comprised of a flat surface of reflecting elements and a horn antenna acting as feed. The reflectarray elements are characterized by a 2×2 complex matrix of reflection coefficients that relate the tangential incident field on the reflectarray surface generated by the horn and the tangential reflected field. The unit cell employed in this work is shown in Fig. 2. It is comprised of two sets of parallel and coplanar dipoles in two layers of metallization, with four dipoles per set. The dipoles oriented along the $\hat{x}_r$ axis control the phase-shift for vertical (V) polarization, while the dipoles oriented along the $\hat{y}_r$ do the same for horizontal (H) polarization. It must be noted that the phase-shift is mainly produced by varying the dipole lengths, so the rest of the parameters are usually fixed (for the present work, separation centre-to-centre between dipoles 3.9 mm and dipole width of 0.5 mm). Thus, up to eight DoF per element are available for the reflectarray design. This unit cell is electromagnetically characterized by the method of moments based on local periodicity (MoM-LP) presented in [18]. This MoM-LP analysis technique has been validated by means of full-wave simulations and measurements of prototypes [18]–[20].

Once the reflected tangential field has been obtained, the far field can be easily calculated by applying the Fourier transform to obtain the spherical components. For an efficient computation of the Fourier transform, the fast Fourier transform (FFT) algorithm may be employed [6]. Then, the copolar and crosspolar components are calculated. For its use in a broadband optimization procedure, the analysis described in [14] is carried out independently at a number of frequencies within a specified band.

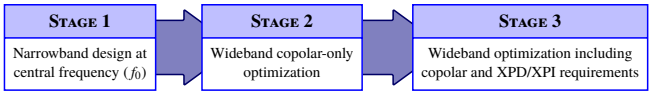

FIGURE 3. **Flowchart of the wideband design procedure. Specifications on the copolar pattern are imposed in all stages, while the cross-polarization requirements are only considered in the last stage of design.**

B. BROADBAND DESIGN PROCEDURE

The broadband design procedure is based on the generalized Intersection Approach (gIA) [21] particularized for reflectarray antennas [14], [22] and extended to dual-band with narrow transmit and received bands in [16]. Thus, no detailed explanation will be provided here, only an overview of the methodology with the new extension developed for this work to achieve broadband performance with high polarization purity in the entire band.

The design methodology is divided into three stages, as shown in Fig. 3. The first stage consists in designing the reflectarray antenna at central frequency. To that purpose, a phase-only synthesis (POS) is carried out independently for each linear polarization. During this step, only copolar specifications are imposed since the POS is based on a simplified analysis, in which the reflectarray unit cell is modelled as an ideal phase-shifter (i.e., with no losses and no cross-polarization). In addition, only one DoF per cell is considered, i.e., the phase of the corresponding complex direct reflection coefficient. This in turn makes the POS computationally very efficient since algorithms based on the use of the FFT may be used [6]. The result of the POS is two phase-shift distributions, one for each linear polarization, that properly tune the impinging field to generate the desired radiation pattern. The layout of the reflectarray is then obtained by adjusting the length of the dipoles, element by element, so they produce the required phase-shift. This reflectarray design complies with the copolar requirements in a narrow band around the frequency of design. In addition, since no cross-polarization requirements were imposed in the process, it may not meet them even at that frequency.

The following step is to carry out a wideband optimization imposing only copolar specifications. This is done at a number of frequencies within that band. To that end, the cost function in the backward projection of the gIA is:

$$F = \sum_{f=1}^{N_f} \left\{ W_f(\vec{r}) \left[\mathrm{CP}'_{\min,f}(\vec{r}) - \mathrm{CP}_{\min,f}(\vec{r};\bar{\xi}) \right] \right\}^2, \qquad (1)$$

where N_f is the total number of frequencies considered in the optimization procedure; W_f is a weighting function that depends on the frequency and an observation point $\vec{r}$ in the coverage zone; $\mathrm{CP}'_{\min,f}(\vec{r})$ is the reference minimum copolar

TABLE 1. Summary of the optimized polarizations, number of degrees of freedom (DoF) and variables considered at each stage and sub-stage of the wideband design procedure. DoF and variables are per unit cell.

Stage	Substage	Polarization(s)	# DoF	Variables
1	1.1	X	1	Phase-shift for pol. X
	1.2	Y	1	Phase-shift for pol. Y
2	2.1	X	1	T_x
	2.2	Y	1	T_y
	2.3	X & Y	2	T_x, T_y
3	3.1	X	3	$T_{x_i}, i = 1, 2, 3$
	3.2	Y	3	$T_{y_i}, i = 1, 2, 3$
	3.3	X & Y	6	$T_{x_i}, T_{y_i}, i = 1, 2, 3$

gain in the coverage zone; $\mathrm{CP}_{\min,f}(\vec{r};\bar{\xi})$ is the current minimum copolar gain in the coverage zone generated by the reflectarray; and $\bar{\xi}$ is the vector of variables, T_x and T_y for this stage. Since now it is necessary to know the frequency response of the unit cell, the MoM-LP will be directly used in the optimization procedure. In addition, in order to facilitate convergence of the algorithm towards a broadband performance, a limited number of DoF per reflectarray element will be used at this stage to carry out the optimization. This is done to reduce the number of local minima in the search space, which mainly depend on the number of DoF for non-convex optimization. Following Fig. 2, we consider two variables per element, T_x and T_y, which are defined as $L_{a_4} = T_x$, $L_{b_1} = L_{b_3} = 0.63T_x$, $L_{b_2} = 0.93T_x$, $L_{b_4} = 0.95T_y$, $L_{a_1} = L_{a_3} = 0.58T_y$, $L_{a_2} = T_y$.

For the final step in the optimization procedure, apart from the copolar requirement, cross-polarization specifications are imposed. For broadcasting applications, two figure-of-merit parameters are usually considered. On the one hand, the crosspolar discrimination (XPD) is defined as the ratio, point by point, of the copolar and crosspolar gains for the coverage area and it is the figure of merit in transmission. Usually its minimum value ($\mathrm{XPD}_{\min}$) is considered, since it is the one limiting the XPD performance. On the other hand, the crosspolar isolation (XPI) is defined as the ratio between the minimum copolar gain and the maximum crosspolar gain in the coverage area and it is the figure of merit for reception. Since the XPI is a stricter parameter than the $\mathrm{XPD}_{\min}$, the XPI will be optimized following the procedure described in [22]. In this way, we ensure that both $\mathrm{XPD}_{\min}$ and XPI will improve. Thus, the cost function in the backward projector is extended to include this parameter:

$$F = \sum_{f=1}^{N_f} \Big\{ W_{f,1}(\vec{r}) \left[\mathrm{CP}'_{\min,f}(\vec{r}) - \mathrm{CP}_{\min,f}(\vec{r};\bar{\xi}) \right] + W_{f,2}(\vec{r}) \left[\mathrm{XPI}'_f(\vec{r}) - \mathrm{XPI}_f(\vec{r};\bar{\xi}) \right] \Big\}^2, \quad (2)$$

Moreover, the number of DoF is increased, to allow for further improvement of the reflectarray performance. Now, the DoFs are the lengths of all dipoles but maintaining the cell symmetry with $L_{a_1} = L_{a_3}$ and $L_{b_1} = L_{b_3}$ (see Fig. 2), i.e. $T_{x_1} = L_{b_1} = L_{b_3}$, $T_{x_2} = L_{b_2}$, $T_{x_3} = L_{a_4}$, $T_{y_1} = L_{a_1} = L_{a_3}$, $T_{y_2} = L_{a_2}$, $T_{y_3} = L_{b_4}$.

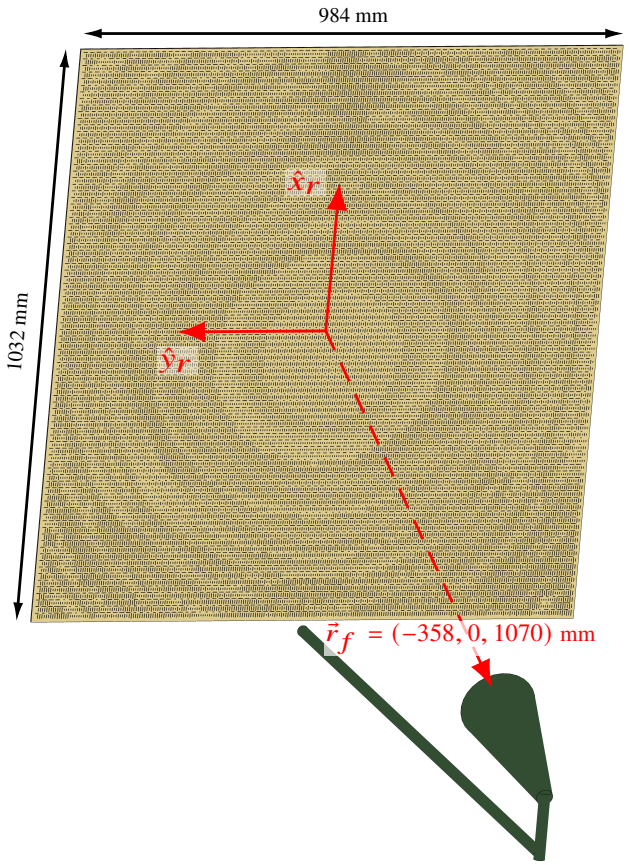

FIGURE 4. Antenna structure employed in this work based on a single-offset configuration.

Finally, a new extension is added in this work to further facilitate convergence towards a wideband performance with improved cross-polarization performance. In addition to the tasks described for stages two and three, each stage is divided into three sub-stages. The first two consist in optimizing only the dipoles of a given linear polarization, and in the third sub-stage both polarizations are optimized at the same time. The benefit of following this strategy is two-fold. On the one hand, each polarization is controlled by a subset of dipoles, so the number of optimizing variables is reduced by half, improving computing times. On the other hand, since we are using fewer optimizing variables, the number of local minima is greatly reduced, improving the convergence of the algorithm [21]. Then, both polarizations are optimized at the same time to account for the little coupling between them that there may exist. Table 1 summarizes, for all stages and their corresponding sub-stages, the optimized polarizations, number of DoF and the variables of the unit cell corresponding to the dipole lengths that are optimized.

III. RESULTS FOR A REFLECTARRAY WITH EUROPEAN COVERAGE

TABLE 2. Minimum EIRP ($EIRP_{min}$, for $P_t = 18$ dBW) and cross-polarization performance (XPD_{min} and XPI) for both linear polarizations (V and H) at seven frequencies in two different stages (stage 1: initial design; stage 3: after cross-polarization optimization).

		10.65 GHz		10.95 GHz		11.40 GHz		11.85 GHz		12.30 GHz		12.75 GHz		13.05 GHz	
		V	H	V	H	V	H	V	H	V	H	V	H	V	H
$EIRP_{min}$ (in dBW)	**Stage 1**	40.84	36.11	42.88	39.88	45.09	43.88	48.21	48.15	47.12	46.14	44.23	41.61	42.44	39.59
	Stage 3	46.26	46.19	47.04	47.67	47.57	47.25	47.69	47.49	47.67	47.25	47.60	47.05	47.15	46.67
XPD_{min} (in dB)	**Stage 1**	33.25	25.83	33.84	27.77	36.40	31.40	36.09	34.83	33.16	33.84	32.93	32.44	33.28	31.84
	Stage 3	39.56	39.63	39.97	39.87	39.36	39.42	38.96	39.21	39.48	39.55	39.83	39.83	39.88	39.85
XPI (in dB)	**Stage 1**	28.50	22.01	29.83	24.83	33.34	28.95	35.75	33.71	31.59	30.42	28.53	24.35	26.34	21.71
	Stage 3	39.22	39.22	39.86	39.84	38.59	37.87	38.55	38.88	39.07	39.35	39.51	39.83	39.49	39.55

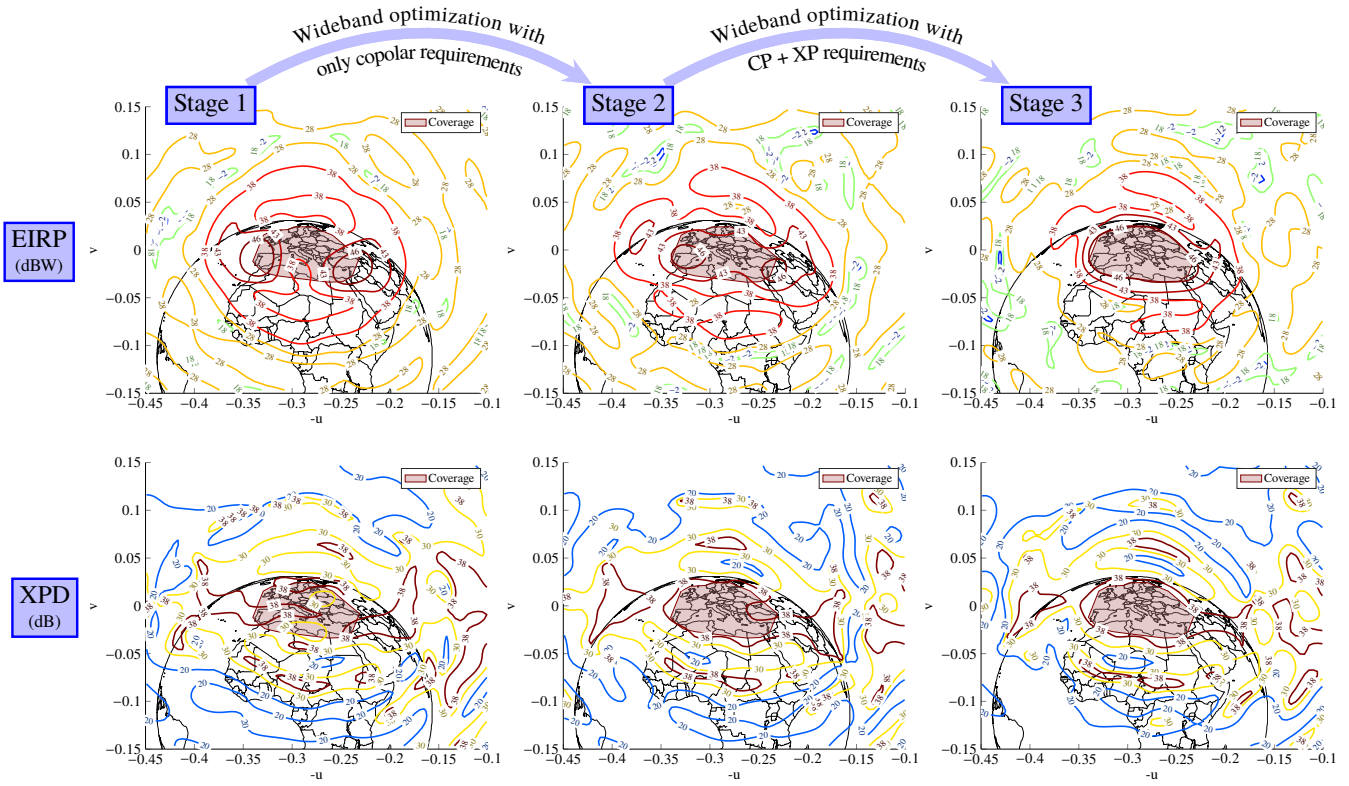

FIGURE 5. For H polarization at 10.65 GHz, EIRP for the copolar pattern (top) and crosspolar discrimination (XPD) (bottom) for the initial design at central frequency and simulated at 10.65 GHz (left), after the broadband copolar-only optimization with a limited number of degrees of freedom (middle), and after the broadband cross-polarization optimization (right).

A. ANTENNA DEFINITION AND REQUIREMENTS

The structure of the antenna is shown in Fig. 4 and it is based on a single-offset configuration. The considered reflectarray is rectangular and it is comprised of 86×82 elements in a regular grid, with a total of 7052 unit cells. The periodicity is $p_x = p_y = 12$ mm, giving an aperture size of $40\lambda_0$ at central frequency (11.85 GHz), with $F/D = 1$ and a clearance of $0.15\lambda_0$. In addition, for the feed a standard 20 dBi Gaussian horn antenna from Flann Microwave is employed. The feed was measured in an anechoic chamber and a $\cos^q\theta$ model [23] is employed, fitting the model to the measured radiation patterns at different frequencies of operation. The horn generates an illumination taper that varies with frequency and ranges from −13.3 dB to −27.6 dB between 10.65 GHz and 13.05 GHz and its phase centre is placed at $\vec{r}_f = (-358, 0, 1070)$ mm with regard to the reflectarray centre.

For the unit cell, since the phase-shift is controlled by the dipole lengths, some of the features are fixed. In the present case, the width of the dipoles is 0.4 mm and the separation center to center between them is set to 4 mm. The substrate for the bottom layer is the commercially available Arlon AD255C ($\varepsilon_{r_A} = 2.55$, $\tan\delta_A = 0.0013$, $h_A = 93$ mil) while for the top layer the substrate is the Diclad 880 ($\varepsilon_{r_B} = 2.17$, $\tan\delta_B = 0.0009$, $h_B = 60$ mil).

In addition, the same European footprint of [15] has been chosen, and it is shown in Fig. 1. It is referred to a geostationary satellite in position 10° E longitude, 0° latitude. The

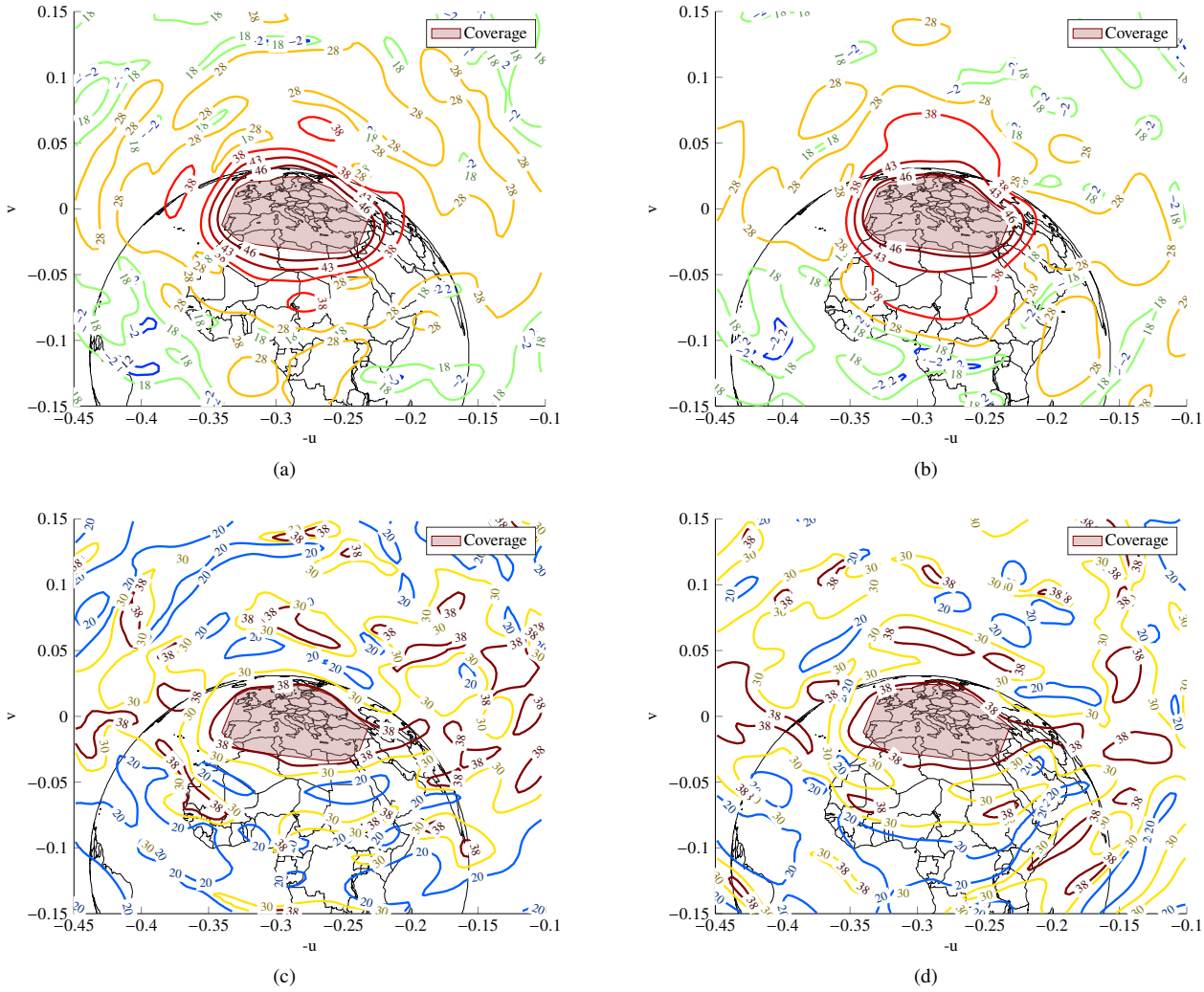

FIGURE 6. Radiation pattern of the optimized reflectarray for H polarization at (a), (c) 11.85 GHz and (b), (d) 13.05 GHz showing the (a), (b) EIRP (dBW) and (c), (d) crosspolar discrimination (dB).

inner contour corresponds to the original specification, but in this work it is enlarged by considering typical pointing errors (0.1° in roll, 0.1° in pitch, and 0.5° in yaw). The minimum copolar requirement is 28 dBi for the enlarged coverage in the frequency band 10.65 GHz–13.05 GHz. With the current technology, the antenna port usually presents values between 17 dBW and 19 dBW of available power. Thus, choosing 18 dBW as a typical value, it gives a minimum effective isotropic radiated power (EIRP) of 46 dBW for the copolar requirement. The goal for cross-polarization performance is to achieve a XPI of at least 30 dB for both linear polarizations in the 20% frequency band.

B. RESULTS

The initial design was carried out at central frequency (11.85 GHz). It was checked that at that frequency the minimum EIRP in the coverage zone was 48 dBW in both polarizations. However, at this first stage the specification of 46 dBW was not met at other frequencies, especially at extreme frequencies, where the minimum EIRP was 36 dBW at 10.65 GHz and 39 dBW at 13.05 GHz. Thus, a wideband optimization is necessary.

The result of this optimization following stages 2 and 3 of Fig. 3 is a considerable improvement in cross-polarization performance while achieving a 100% compliance in EIRP (at least 46 dBW) in a 20% bandwidth in dual-linear polarization. The worse XPD_{min} and XPI are 39.0 dB and 37.9 dB, for V polarization at 11.85 GHz and H polarization at 11.40 GHz, respectively. It is worth noting that the XPI parameter for H polarization at 13.05 GHz improved more than 17 dB, from a value of 21.7 dB for the initial design at central frequency to a value of 39.5 dB after the cross-polarization optimization. Considering the worst cases for the initial and optimized reflectarrays for all frequencies and polarizations, the XPD_{min} has improved more than 13 dB (from 25.8 dB for H polarization at 10.65 GHz to 39.0 dB for V polarization at 11.85 GHz) and the XPI has improved more than 16 dB (from 21.7 dB for H polarization at 13.05 GHz to

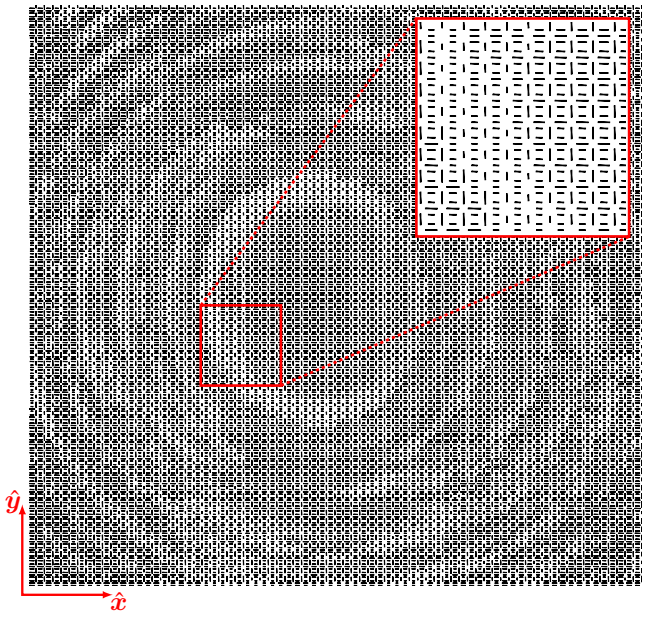

FIGURE 7. Mask layout of the bottom layer of the optimized broadband reflectarray with European coverage.

37.9 dB for H polarization at 10.95 GHz). Table 2 gathers the values of the minimum EIRP, XPD_{min} and XPI for both linear polarizations and seven frequencies in a 20% bandwidth for the initial (stage 1) and optimized (stage 3) layouts.

Fig. 5 shows the EIRP and XPD for H polarization at 10.65 GHz for the three stages of the optimization. This polarization and frequency represent the worse case at the starting point, since the minimum EIRP is 36.1 dBW, representing a compliance of 22.1%, while the XPD_{min} and XPI have values of 25.8 dB and 22.0 dB, respectively. This value of the XPD_{min} is the worst in the whole band, while the XPI represents the second worst, only 0.3 dB higher than the XPI for H polarization at 13.05 GHz, as shown in Table 2. After the broadband copolar-only optimization (stage 2), the minimum EIRP in the coverage area improves to a value of 41.6 dBW, which is an improvement of 5.5 dB over the initial design. At this stage, it is still the worse case for the copolar pattern. On the other hand, the cross-polarization parameters improve, having values higher than 30 dB. In fact, the XPD_{min} is 35.1 dB while the XPI is 31.9 dB. The final optimization improves the EIRP and now it complies with the 46 dBW specification in the whole coverage area, while the XPD_{min} and XPI reach values better than 37.9 dB. Fig. 6 shows the EIRP and XPD at central (11.85 GHz) and upper (13.05 GHz) frequencies of the optimized reflectarray, while Fig. 7 shows the layout of the optimized broadband reflectarray with European coverage and improved cross-polarization performance.

C. DESIGN PRECISION AND DRIFT TOLERANCE STUDY

A study was carried out to test the tolerance of the design to small modifications in the size of the reflectarray elements.

TABLE 3. Comparison of the presented design with other works in the literature in terms of relative bandwidth and cross-polarization performance.

Work	BW	CP_{min}	XPD_{min}	XPI_{min}
[15]	15%	28.0 dBi	—	30 dB (in a 9.2% BW)
[13]	20%	26.4 dBi	24.1 dB	—
Here	20%	28.2 dBi	39.0 dB	37.9 dB

First, a loss of precision of 200 μm was considered in the length of the dipoles. In this case, the variation of the minimum EIRP is smaller than 0.22 dB and still complies with specifications for both polarizations in the whole frequency band. It affects more to higher frequencies, where the minimum EIRP diminishes between 0.12 dB and 0.21 dB. Regarding the cross-polarization performance, higher frequencies are more affected as well, but the decrease in XPD_{min} and XPI is smaller than 0.4 dB, and the worse values are still better than 37.8 dB for both parameters.

A drift of $\pm 50\,\mu$m was also considered in the dipole lengths. The drift penalizes more the performance of the reflectarray. For the minimum EIRP, the worse case is produced at 13.05 GHz with a decrease of 0.33 dB. However, it still complies with specifications for both polarizations in the 20% bandwidth. In the case of the cross-polarization parameters, there is a decrease up to 0.9 dB for the XPI at 12.30 GHz. However, the minimum values for both polarizations in the whole band are still better than 37.5 dB.

Since the antenna works in dual-linear polarization, the improvement of the polarization purity by maximizing the XPD and XPI parameters allows to reduce the interference of one polarization over the other, increasing the signal-to-interference-plus-noise ratio. This would allow to employ modulations with better spectral efficiency, improving the transmitted data rate.

Finally, it is worth mentioning that the reflectarray design presented in this work outperforms other works in the literature, as reviewed in the Introduction, in terms of bandwidth and cross-polarization performance. Table 3 compares, in terms of bandwidth and cross-polarization performance, the presented design in this work and others in the literature with similar European coverage. The improved performance has been achieved thanks to the tightly controlled broadband design procedure, divided in several stages and sub-stages to control convergence towards a high-performance design.

IV. CONCLUSIONS

This work demonstrates the capability of high-performance reflectarray antennas to provide service for space applications in a large bandwidth with stringent cross-polarization requirements. The large bandwidth allows to provide more channels for UHDTV broadcasting while the high polarization purity allows to obtain a better signal-to-interference-plus-noise ratio, which in turn enables to use modulations with improved spectral efficiency. The broadband de-

sign procedure is divided in several stages and sub-stages. Each successive stage makes the constraints increasingly tighter while adding more DoF. These stages are in turn divided into sub-stages, in which the orthogonal polarizations are optimized independently. The aim of this strategy is to tightly control the algorithm in order to facilitate convergence towards a broadband performance with enhanced polarization purity. This procedure was applied to the design of a 1-meter broadband reflectarray with European coverage. The antenna is dual-linear polarized and works in a 20% bandwidth in X-Ku bands (10.65 GHz–13.05 GHz). After the optimization, the reflectarray is able to provide at least 46 dBW of EIRP (assuming 18 dBW of available power in the antenna port) in the coverage area while presenting a cross-polarization performance better than 37 dB in the 20% bandwidth, outperforming other designs in the literature in terms of bandwidth and cross-polarization. This methodology may be readily extended to include dual-circular polarization.

References

[1] C. Sacchi, T. Rossi, M. Murroni, and M. Ruggieri, "Extremely high frequency (EHF) bands for future broadcast satellite services: Opportunities and challenges," IEEE Trans. Broadcast., vol. 65, no. 3, pp. 609–626, Sep. 2019.

[2] M. Kojima, Y. Suzuki, Y. Koizumi, and H. Sujikai, "Transmission experiments for 32APSK by digital pre-distortion over satellite simulator," in IEEE Radio and Wireless Symposium (RWS), Orlando, Florida, USA, Jan. 20–23, 2019, pp. 1–3.

[3] M. Nagasaka, S. Nakazawa, M. Kojima, and S. Tanaka, "Prototype of 12/21 GHz-band dual-circularly polarized receiving antenna for satellite broadcasting," in Asia-Pacific Microwave Conference (APMC), Kyoto, Japan, Nov. 6–9, 2018, pp. 1163–1165.

[4] H. Yamamoto, A. Nakamura, and M. Itami, "A study on LDM-BST-OFDM transmission for the next-generation terrestrial broadcasting," IEEE Trans. Broadcast., pp. 1–11, 2019, early access.

[5] W. A. Imbriale, S. Gao, and L. Boccia, Eds., Space Antenna Handbook. Hoboken, NJ, USA: John Wiley & Sons, 2012.

[6] J. Huang and J. A. Encinar, Reflectarray Antennas. Hoboken, NJ, USA: John Wiley & Sons, 2008.

[7] J. A. Encinar and J. A. Zornoza, "Three-layer printed reflectarrays for contoured beam space applications," IEEE Trans. Antennas Propag., vol. 52, no. 5, pp. 1138–1148, May 2004.

[8] E. Carrasco, J. A. Encinar, and M. Barba, "Bandwidth improvement in large reflectarrays by using true-time delay," IEEE Trans. Antennas Propag., vol. 56, no. 8, pp. 2496–2503, Aug. 2008.

[9] J. H. Yoon, Y. J. Yoon, W. sang Lee, and J. ho So, "Broadband microstrip reflectarray with five parallel dipole elements," IEEE Antennas Wireless Propag. Lett., vol. 14, pp. 1109–1112, 2015.

[10] D. M. Pozar, "Wideband reflectarrays using artificial impedance surfaces," Electron. Lett., vol. 43, no. 3, pp. 148–149, Feb. 2007.

[11] V. Richard, R. Loison, R. Gillard, H. Legay, M. Romier, J.-P. Martinaud, D. Bresciani, and F. Delepaux, "Spherical mapping of the second-order phoenix cell for unbounded direct reflectarray copolar optimization," Progr. Electromagn. Res. C, vol. 90, pp. 109–124, 2019.

[12] M. Zhou, S. B. Sørensen, O. S. Kim, E. Jørgensen, P. Meincke, and O. Breinbjerg, "Direct optimization of printed reflectarrays for contoured beam satellite antenna applications," IEEE Trans. Antennas Propag., vol. 61, no. 4, pp. 1995–2004, Apr. 2013.

[13] M. Zhou, S. B. Sørensen, O. S. Kim, E. Jørgensen, P. Meincke, O. Breinbjerg, and G. Toso, "The generalized direct optimization technique for printed reflectarrays," IEEE Trans. Antennas Propag., vol. 62, no. 4, pp. 1690–1700, Apr. 2014.

[14] D. R. Prado, M. Arrebola, M. R. Pino, R. Florencio, R. R. Boix, J. A. Encinar, and F. Las-Heras, "Efficient crosspolar optimization of shaped-beam dual-polarized reflectarrays using full-wave analysis for the antenna element characterization," IEEE Trans. Antennas Propag., vol. 65, no. 2, pp. 623–635, Feb. 2017.

[15] J. A. Encinar, M. Arrebola, M. Dejus, and C. Jouve, "Design of a 1-metre reflectarray for DBS application with 15% bandwidth," in First European Conference on Antennas and Propagation (EuCAP), Nice, France, Nov. 6–10, 2006, pp. 1–5.

[16] D. R. Prado, M. Arrebola, M. R. Pino, and G. Goussetis, "Contoured-beam dual-band dual-linear polarized reflectarray design using a multi-objective multi-stage optimization," IEEE Trans. Antennas Propag., 2020, accepted.

[17] C. I. Kourogiorgas, D. Tarchi, A. Ugolini, P. D. Arapoglou, A. D. Panagopoulos, G. Colavolpe, and A. V. Coralli, "System capacity evaluation of DVB-S2X based medium earth orbit satellite network operating at Ka band," in 8th Advanced Satellite Multimedia Systems Conference and the 14th Signal Processing for Space Communications Workshop (ASMS/SPSC), Palma de Mallorca, Spain, Sep. 5–7, 2016, pp. 1–8.

[18] R. Florencio, R. R. Boix, J. A. Encinar, and G. Toso, "Optimized periodic MoM for the analysis and design of dual polarization multilayered reflectarray antennas made of dipoles," IEEE Trans. Antennas Propag., vol. 65, no. 7, pp. 3623–3637, Jul. 2017.

[19] E. Martinez-De-Rioja, J. A. Encinar, R. Florencio, and C. Tienda, "3-d bifocal design method for dual-reflectarray configurations with application to multibeam satellite antennas in Ka-band," IEEE Trans. Antennas Propag., vol. 67, no. 1, pp. 450–460, Jan. 2019.

[20] D. Martinez-De-Rioja, E. Martinez-De-Rioja, J. A. Encinar, R. Florencio, and G. Toso, "Reflectarray to generate four adjacent beams per feed for multispot satellite antennas," IEEE Trans. Antennas Propag., vol. 67, no. 2, pp. 1265–1269, Feb. 2019.

[21] O. M. Bucci, G. D'Elia, G. Mazzarella, and G. Panariello, "Antenna pattern synthesis: a new general approach," Proc. IEEE, vol. 82, no. 3, pp. 358–371, Mar. 1994.

[22] D. R. Prado and M. Arrebola, "Effective XPD and XPI optimization in reflectarrays for satellite missions," IEEE Antennas Wireless Propag. Lett., vol. 17, no. 10, pp. 1856–1860, Oct. 2018.

[23] Y.-T. Lo and S.-W. Lee, Eds., Antenna Handbook Vol. 1. New York, NY, USA: Van Nostrand Reinhold, 1993, ch. 1, pp. 28–29.